Research Square

Preprints are preliminary reports that have not undergone peer review.
They should not be considered conclusive, used to inform clinical practice,
or referenced by the media as validated information.

First Application of a Ball-Pen Probe for Direct Measurements of Plasma Potential and Nonlinear Fluctuations Dynamics in a Linear Helicon Plasma

Donato Di Matteo
Kyushu University
Jiri Adamek
Czech Academy of Sciences, Institute of Plasma Physics
Jordan Cavalier
Czech Academy of Sciences, Institute of Plasma Physics
Yoshihiko Nagashima
Kyushu University
Takuma Yamada
Kyushu University
Ren Namimatsu
Kyushu University
Huiwon Chung
Seoul National University
Chanho Moon
moon@riam.kyushu-u.ac.jp

Kyushu University

Article

Keywords:

Posted Date: August 20th, 2026

DOI: https://doi.org/10.21203/rs.3.rs-10597406/v1

License: This work is licensed under a Creative Commons Attribution 4.0 International License.
Read Full License

Additional Declarations: No competing interests reported.

First Application of a Ball-Pen Probe for Direct Measurements of Plasma Potential and Nonlinear Fluctuations Dynamics in a Linear Helicon Plasma

D. Di Matteo[1], J. Adamek[4], J. Cavalier[4], Y. Nagashima[2,3], T. Yamada[3,5],
R. Namimatsu[1], H. Chung[6], and C. Moon[* 2,3]

[1]*Interdisciplinary Graduate School of Engineering Sciences, Kyushu University, Kasuga 816-8580, Japan*
[2]*Research Institute for Applied Mechanics, Kyushu University, Kasuga 816-8580, Japan*
[3]*Research Center for Plasma Turbulence, Kyushu University, Kasuga 816-8580, Japan*
[4]*Institute of Plasma Physics of the CAS, Prague, 18200, Czech Republic*
[5]*Faculty of Arts and Science, Kyushu University, Fukuoka 819-0395, Japan*
[6]*Department of Nuclear Engineering, Seoul National University, Seoul 08826, Republic of Korea*

Abstract

Direct measurements of the plasma space potential and electron temperature are essential for characterizing plasma dynamics and fluctuations, particularly in magnetized plasma systems. Here, a ball-pen probe (BPP) is assembled and installed for the first time on a linear helicon plasma device, enabling direct and fast measurements of the plasma space potential and, in combination with a Langmuir probe, the electron temperature. A comparative study between BPP and Langmuir probe measurements demonstrates the success of the BPP in simultaneously resolving radial profiles and temporal fluctuations of the plasma potential and electron temperature. Preliminary measurements further reveal low-frequency instabilities and nonlinear plasma potential dynamics that are not directly accessible through Langmuir probe measurements. These results demonstrate for the first time the potential of BPPs for direct investigation of plasma potential dynamics and turbulence in linear helicon plasmas.

[*] Electronic mail: moon@riam.kyushu-u.ac.jp

1. Introduction

Understanding anomalous turbulent transport mechanisms in magnetized plasmas is essential for improving plasma confinement in fusion devices [1-3] and enhancing performance and efficiency in plasma propulsion systems such as electric thrusters [4-6]. In plasma turbulence studies, direct measurements of the plasma space potential (ϕ_s) and electron temperature (T_e) are crucial for evaluating quantities such as electric field fluctuations, heat flux and particle flux [7-9], which must be controlled during the operation of magnetically confined plasma systems. However, plasma potential is still a relatively difficult quantity to measure and several diagnostics have been developed for this purpose, including heavy ion beam probe [10], emissive probe [11] and ball-pen probe (BPP), which is the subject of this study. Nonetheless, in many experiments, floating potential fluctuations measured by Langmuir probes (LP) are still used as a proxy for plasma potential fluctuations [12]. In this context, linear plasma devices remain valuable systems for turbulence and transport studies due to their simplified geometry, broad diagnostic accessibility, high degree of experimental control and reproducibility. Among linear devices, helicon sources are particularly attractive because they can generate high-density linear plasmas under steady-state operation [13, 14].

The ball-pen probe, an electrostatic probe designed by Adamek *et al.* [15] as an evolution of the Katsumata probe concept [16], enables direct measurements of ϕ_s and T_e in magnetized plasmas [17-18], as well as measurements of T_i [19, 20]. It has been successfully used in several high-temperature [21-23] and low-temperature [24-26] plasma devices. It is based on a simple and robust design, does not require external biasing, and minimally perturbs the plasma. The BPP consists of a metal collector which can be inserted in a non-conductive shielding tube. In well-magnetized plasma, the operating principle of the BPP relies on the difference in the gyromotion properties between electrons and ions. The opposite gyration direction of electrons and ions around the magnetic field lines generates a cross-field transport mechanism that drives charged particles into the shielding tube [27]. By appropriately retracting the collector inside the tube, the collection of electrons is preferentially reduced because their Larmor radius is much smaller than that of the heavier ions. Electrons hit the shielding wall, while ions can still reach the collector. Therefore, the electron saturation current I_{sat}^- is reduced, while the ion

saturation current I_{sat}^{+} is only weakly affected. The probe floating potential, defined by the condition of zero net collected current, shifts toward more positive values as the electron current decreases. When the electron and ion saturation currents become comparable, the floating potential ϕ_{f} of the BPP approaches the plasma space potential ϕ_{s}, as follows from Eq. (1).

However, in weakly-magnetized plasmas, collisions and cross-field drift phenomena appear to play a more significant role in the collection of ions and electrons, with their impact mainly depending on the degree of ion magnetization. The operating conditions of the present study fall within this regime. A complete understanding of BPP mechanism in such plasmas has yet to be established.

For a Maxwellian plasma, the characteristic relation between the ϕ_{s} and the ϕ_{f} of an electrostatic probe is given by the following [28]:

$$\phi_{\mathrm{s}} = \phi_{\mathrm{f}} + \alpha T_{\mathrm{e}} \;=\; \phi_{\mathrm{f}} + \ln\left(\frac{I_{\mathrm{sat}}^{-}}{I_{\mathrm{sat}}^{+}}\right) T_{\mathrm{e}} =\; \phi_{\mathrm{f}} + \ln(R)\, T_{\mathrm{e}}, \tag{1}$$

where R is the ratio between I_{sat}^{-} and I_{sat}^{+}, $\alpha = \ln(R) = \ln\left(\frac{I_{\mathrm{sat}}^{-}}{I_{\mathrm{sat}}^{+}}\right)$, T_{e} is the electron temperature expressed in eV. By combining this equation for both BPP and LP, the electron temperature can also be directly estimated by knowing both α_{BPP} and α_{LP}:

$$T_{\mathrm{e}} = \frac{\phi_{\mathrm{f,BPP}} - \phi_{\mathrm{f,LP}}}{\alpha_{\mathrm{LP}} - \alpha_{\mathrm{BPP}}} \;. \tag{2}$$

This approach lastly leads to the possibility of using ϕ_{s} and T_{e} fast measurements to evaluate electric fields and fluctuations-driven heat and particle fluxes.

A feasibility study of a new BPP installed in the Plasma Assembly for Non-linear Turbulence Analysis device (PANTA) has been conducted to investigate the applicability of BPP in high-density linear helicon plasmas, where the BPP has been implemented for the first time. Preliminary measurements of ϕ_{s}, T_{e} and relative fluctuations are performed. Main goal for the use of BPP is exploiting its potential to reveal plasma potential fluctuation information inaccessible to previously used diagnostics, as this can contribute to resolve fluctuations-based phenomena in various applied plasma studies. The present work provides a preliminary assessment of this capability.

2. Experimental Setup

The reported experiments are carried out in the PANTA device [29] at Kyushu University. A schematic of this device is shown in Fig. 1(a). PANTA has a vacuum vessel with z-axial length of 4 m and diameter of 0.45 m. Helmholtz coils surrounding the vessel can generate a magnetic field of up to 150 mT. Base vacuum pressure is of the order of 10^{-4} Pa. Typical plasma discharges have a duration of 0.6 s. An analog-to-digital conversion (ADC) system with a sampling frequency of 1 MHz is used for the measurements. Data are collected shot by shot.

The plasma used in this study is generated in the source chamber from Argon gas, which is ionized by a double loop helicon antenna operating at 7 MHz with an input power of 3 kW. The antenna has a diameter of 10 cm. The neutral gas pressure is set to 0.36 Pa and a uniform axial magnetic field of B = 100 mT is applied to confine the plasma. Under these operating conditions, PANTA can produce an electron density in the range of 10^{18} – 10^{19} m^{-3} and an electron temperature in the 1 – 3 eV interval. Under the present experimental conditions, the average electron Larmor radius ρ_{ce} is approximately 0.06 mm, whereas the average ion Larmor radius ρ_{ci} is approximately 8 mm.

A radially movable probe array is installed via a feedthrough, perpendicularly to the magnetic field

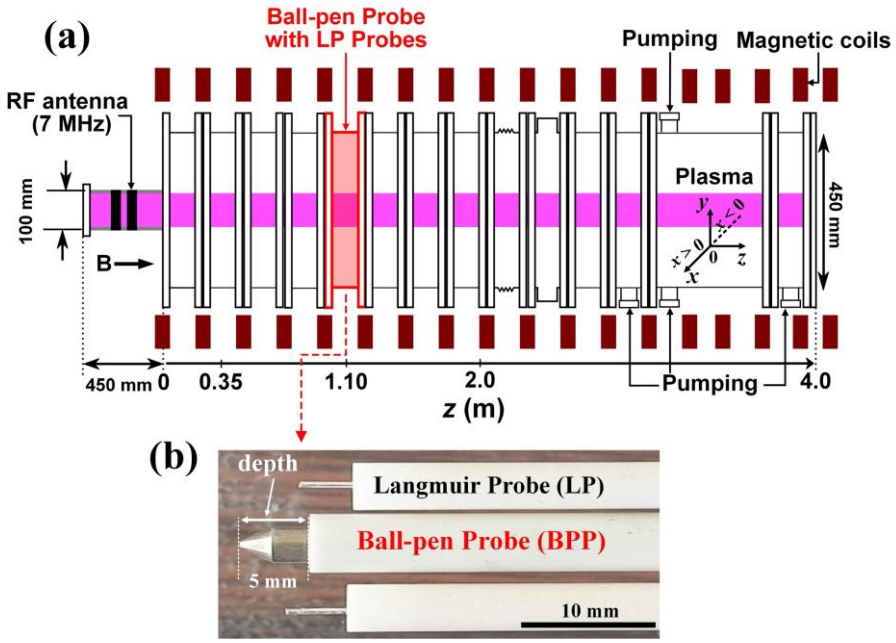


Figure 1. (a) Schematic diagram of the cylindrical magnetized plasma device PANTA, and (b) photography of the probe array with BPP and two LP.

lines, at an axial position of z = 1.1 m from the plasma source, as shown in Fig.1(a). Its radial position is calibrated with a fluctuations-based method involving a coherence analysis with another radially fixed probe [30].

The array consists of one BPP and two LP. The BPP has a stainless-steel collector with a diameter of 3.2 mm and a conical tip. The collector is shielded by an alumina (Al_2O_3) tube with an inner diameter of approximately 3.75 mm and an outer diameter of approximately 5 mm. Both the two LP collectors have a diameter of 0.8 mm.

The BPP collector position can be adjusted perpendicularly to the magnetic field lines, with a resolution of 0.01 mm, through a manual dial on the external body of the probe. However, proper calibration between the physical depth of the collector and the dial reading was not possible in the current setup. Therefore, the dial reading h_d is used as a reference parameter to track the position of the collector relative to the shielding tube. The collector can be moved between dial readings h_d of 0 mm and 25 mm. Higher values correspond to the collector being retracted inside the tube, whereas lower values correspond to the tip of the collector being in the plasma, outside of the shielding tube. Consequently, h_d is hereafter used to denote the collector depth.

Figure 1(b) shows the probe array configuration. The BPP is located at the center, with two LP positioned 5 mm vertically above and below it. One LP is biased using a bipolar power supply that applies a sweep voltage ranging from -50 V to +50 V at a frequency of 50 Hz, allowing the acquisition of I-V characteristic curves. The curves are used to derive reference values of plasma potential and electron temperature using standard Langmuir probe theory [31]. The second LP is operated in a floating configuration, and its floating potential is measured using a high input impedance (~1 MΩ) acquisition system. This measurement is used in combination with the BPP floating potential to determine the electron temperature through Eq. (2). The coefficient $\alpha = \ln\left(\frac{I_{sat}^-}{I_{sat}^+}\right)$ for both the LP and the BPP is determined from experimental I-V curves; The coefficient associated with the Langmuir probe was found to be approximately constant, with a value of about 4 across the plasma radius in PANTA.

III. EXPERIMENTAL RESULTS AND DISCUSSION

A. Optimization of collector depth

Helicon plasmas are characterized by significantly higher densities than common low-temperature linear plasmas. However, as in other low-temperature devices where the BPP has been tested [17, 24-26], the magnetic field in PANTA is not strong enough to fully magnetize argon ions across the entire plasma radius. In the core, where the plasma density reaches its maximum, collisional effects dominate ion dynamics over gyromotion. The combination of high plasma density and limited ion magnetization under typical helicon plasma conditions makes the optimization of the BPP collector depth a critical requirement for accurate plasma potential profile measurements. Since the electron density also significantly changes along the radius (see Fig. 5a), determining the optimal value of the collector depth dial reading h_d is not straightforward. This issue is addressed experimentally as follows.

First, the BPP is operated in sweep mode. An h_d-scan of the I-V characteristic curves is performed at different radial positions across the whole plasma radius. For each position of the collector, 28 I-V curves are collected during a steady-state regime of 300 ms. As no hysteresis phenomena are observed in the I-V curves between successive voltage sweeps, the curves are directly averaged without any

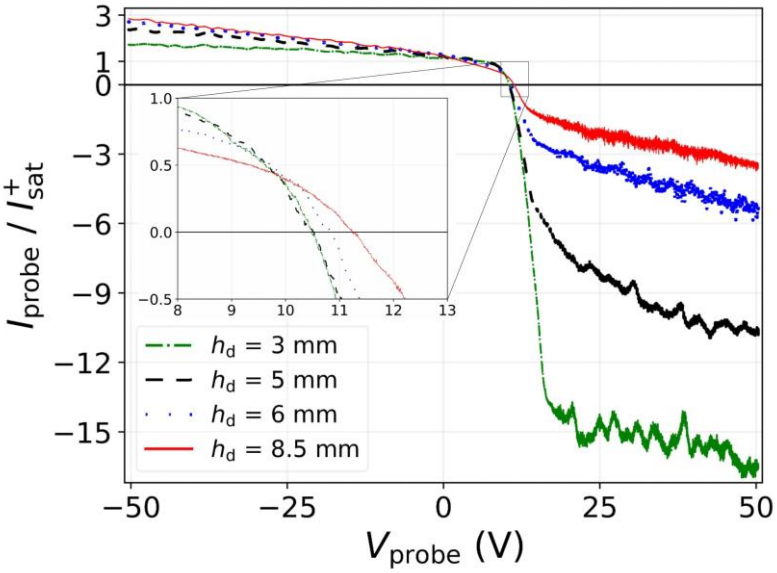


Figure 2. BPP I-V characteristics normalized to I^+_{sat} at r = 5.5 for different collector positions h_d. Larger h_d values correspond to the collector being more retracted inside the shielding tube. The I-V characteristics become increasingly symmetric with increasing h_d, with a corresponding shift in ϕ_f (zoom). The most symmetric profile is observed at h_d = 8.5 mm. Each curve is averaged over 28 I-V sweeps.

concern. Linear fittings are performed in the ion and electron saturation regions and each of the saturation currents is extrapolated from the corresponding fitting at the floating potential. Figure 2 shows the averaged I-V traces of the BPP, normalized to the ion saturation current I_{sat}^{+} for four different values of h_d, at the edge radial position of r = 5.5 cm. At a dial position h_d = 3 mm, the saturation current ratio R of the probe is approximately 15, suggesting that the tip is already slightly outside of the shielding tube. As the collector is progressively retracted inside the tube, the ratio R decreases to almost unity. Eventually, the curve corresponding to h_d = 8.5 mm exhibits a ratio R = 1.42, with an I_{sat}^{+} of approximately 1.21 mA. This confirms that the I-V characteristics successfully approaches a symmetric shape. As expected from the PIC simulations reported by S. Murphy-Sugrue *et al.* [27], the electron branch does not saturate but instead increases approximately linearly with probe bias.

However, for further retraction, the geometric shielding also begins to significantly limit ion access to the collector. Beyond this point, the ion saturation current decreases faster than the electron saturation current, causing R to rapidly increase again after reaching a minimum value close to 1. This is shown in Figure 3, which displays the dependence of the coefficient α_{BPP} (circle markers) and the BPP floating potential (square markers) on the dial reading h_d of the collector depth at r = 5.5 cm. In many

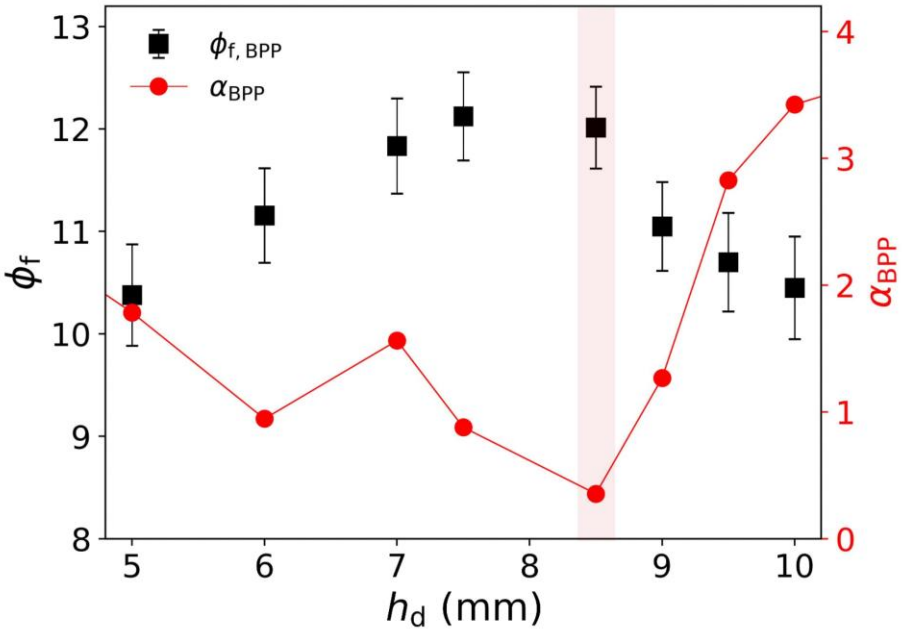


Figure 3. Dependence of the saturation current ratio coefficient α_{BPP} (circles) and the BPP floating potential (squares) on the collector position h_d at r = 5.5 cm. The shaded region denotes the optimal operation range of the BPP.

plasma devices and conditions, a plateau in both R and ϕ_f is typically observed over a wide range of collector retraction values after reaching the minimum R [15, 25, 27]. In the PANTA helicon plasma, however, no such plateau is detected. Instead, the optimal operating condition is confined to a relatively narrow region of the retraction h_d. Only within this region, the BPP floating potential can be considered a reliable estimate of the plasma space potential. This implies that the collector depth must be precisely optimized.

Moreover, it was observed that the optimal value of h_d changes with radial position. This behavior seems to be mainly related to the substantial change in plasma density along the radius, which reaches its maximum on the axis. The plasma density directly influences both the collision frequency and $E \times B$ drift phenomena [27,32].

B. Hall parameter effect

To further interpret the dependance on the electron density radial profile, it can be useful to consider the evolution of particle magnetization along the plasma radius. This can be quantified through the Hall parameter $\beta_{e,i}$, which can be defined, for ions or electrons separately, as the ratio between the cyclotron frequency ω_c and the total collision frequency ν [24]. In low temperature plasmas, weak ion magnetization is quite common and could limit the use of the BPP. In previous work by Zanáška *et al.* [26], this concern led to the conclusion that the BPP becomes operational when the magnetic field to pressure ratio, B/P, exceeds 10 mT Pa^{-1}. In the PANTA conditions investigated in this work, the ratio B/P is approximately 280 mT Pa^{-1}. Nonetheless, the applicability of the BPP in PANTA encounters some limitations in the plasma core, where the particle density is highest. Helicon sources typically generate plasma densities one to two orders of magnitude greater than those of other low-temperature devices operating at similar neutral pressures. This substantially increases the ion collisions frequency and reduce ion magnetization despite the large value of B/P, indicating that under the present experimental conditions the B/P criterion alone is not enough to assess BPP applicability.

Figure 4 shows the radial profiles of the ion Hall parameter β_i and the corresponding saturation current coefficient α_{BPP}. While electrons remain strongly tied to magnetic field lines across the entire

plasma radius, the ion Hall parameter β_i exhibits a strong radial variation due to the increase in plasma density toward the core. In the core region, $\beta_i \ll 1$ and α_{BPP} increases to approximately 2 with a trend similar to the typical PANTA density profile. Toward the plasma edge, the decrease in α_{BPP} is accompanied by increasing ion magnetization. Their opposite trends suggest that α_{BPP} begins to significantly increase at radial positions where ion magnetization becomes particularly weak, indicating a departure from ideal BPP operating conditions. Accordingly, the ion motion becomes collision dominated and the ion collection mechanism is substantially modified. Ions are no longer constrained by magnetic field lines and can enter the shielding tube more easily than the magnetized electrons through collisional transport involving ion–ion and ion–neutral interactions.

As highlighted by Bousselin *et al.* [24], this leads to the formation of a positive space charge near the entrance of the tube. Since the Debye length is much smaller than the tube radius, a strong electric field develops in this region. This field can drive electrons into the shielding tube by $E \times B$ drifts [24, 32], thereby increasing the electron current and preventing the current ratio R from approaching unity. Consequently, in the core, the BPP floating potential could approach the plasma potential if a correction based on the coefficient α_{BPP} is applied.

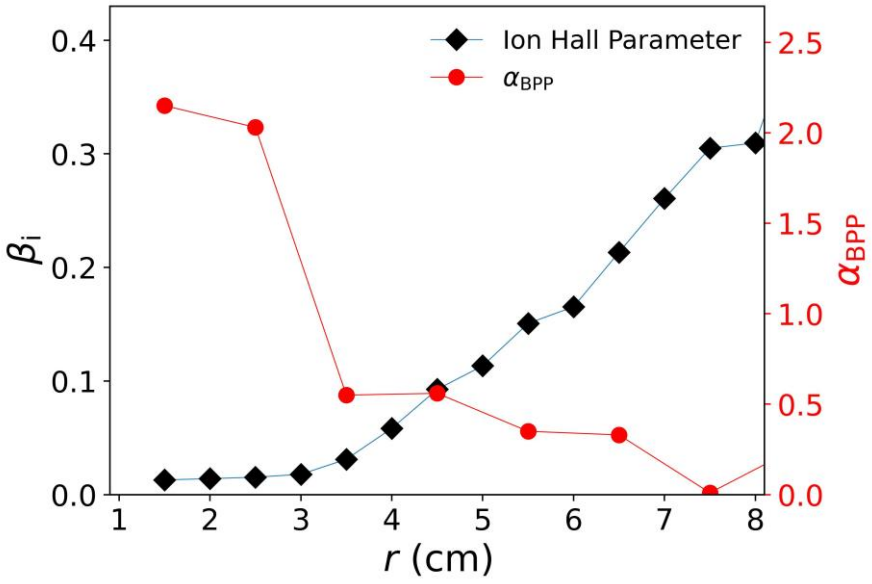


Figure 4. Radial profiles of ion Hall parameter $\beta_i = \omega_{ci}/\nu_i$ (black) and the BPP saturation current ratio coefficient α_{BPP} (red) in the PANTA helicon plasma. The decrease in α_{BPP} towards the plasma edge is accompanied by increasing ion magnetization. In the estimation of ν_i, Ion–ion and ion–neutral collisions were considered, ion–electron collisions were neglected. Ion acoustic velocity was used to calculate the ion-ion collision frequency ν_{ii}.

C. Direct measurements of ϕ_s and T_e

The impact of this behavior on the direct measurements of plasma parameters is illustrated in Fig. 5, which shows the (a) density radial profile and compares the radial profiles of (b) plasma potential and (c) electron temperature obtained from the BPP (circle markers) with those derived from LP I–V characteristics (square markers).

The reference LP measurements of plasma potential are obtained from the semi-logarithmic representation of the LP I-V characteristics, by identifying the intersection between the linear fit to the electron saturation region and the fit to the transition region.

The BPP is operated in a floating potential configuration for direct measurements with the collector depth adjusted to its optimal value at each radial position based on the local minimum of the current ratio R. In addition, a correction equal to $\alpha_{\mathrm{BPP}} T_e$ was applied to the BPP floating potential to account for the non-zero value of α_{BPP}. The electron temperature used for this correction was derived from the BPP measurements, by using Eq. (2). The correction is relevant primarily in the core region, where α_{BPP} more significantly deviates from zero.

When the correction is applied, agreement is observed across the entire plasma radius. At the edge and outer region of the plasma, where β_i remains above approximately 0.1 and the BPP operating conditions are better satisfied, good agreement is observed between the two diagnostics for both plasma potential and electron temperature without any correction. Direct measurements can therefore be used to study particle and heat transport, which depend on the radial electric field and are of particular interest in the edge region.

These results demonstrate the first successful direct measurements of both plasma potential and electron temperature profiles using the BPP in a linear helicon plasma.

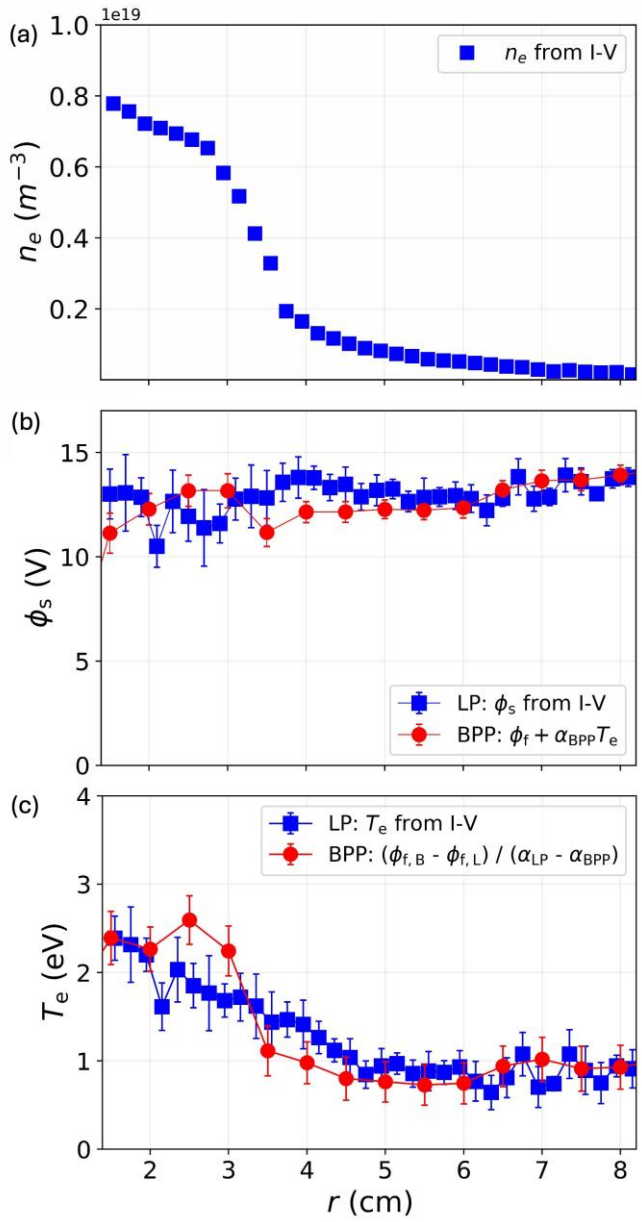


Figure 5. Radial profiles of (a) electron density, (b) space potential and (c) electron temperature obtained with LP (blue) and BPP (red). BPP collector depth has been adapted to its optimal value for each radial position. Error bars denote the standard deviation of the temporal signals (BPP) and of the 28 sweeps used to obtain the averaged I–V curves (LP). Helicon plasma source has a radius of 5 cm.

D. Discussion of low-frequency fluctuations

A preliminary investigation of plasma potential fluctuations was conducted from direct measurements performed by the BPP. These measurements were again compared to Langmuir probe measurements, since LP floating potential fluctuations are commonly used as a proxy for plasma potential fluctuations [12]. However, finite temperature fluctuations introduce spurious contributions to

the Langmuir probe signal, as suggested by Eq. (1). Consequently, in such regimes -particularly over specific frequency ranges where temperature fluctuations may be non-negligible- LP floating potential fluctuations cannot reliably represent plasma potential fluctuations. In contrast, BPP provides direct measurements of plasma potential fluctuations.

The dynamic impedance Z_d of the Ball-pen probe in the PANTA plasma is evaluated through BPP I-V curves to assess whether the probe can detect high-frequency fluctuations. It is found that, across the entire plasma radius, Z_d increases with increasing collector retractions inside the tube. At the radial position $r = 3.5$ cm, the optimal BPP operating condition corresponds to a collector depth $h_d = 8.46$ mm. Under these conditions, Z_d is approximately 1 kΩ. In an ideal case, corresponding to a low system capacitance of approximately 400 pF, this low dynamic impedance would allow the BPP to detect fast fluctuations up to a cutoff frequency of approximately 400 kHz. Under experimental conditions, however, the effective system capacitance may increase by a factor of 5, reducing the cutoff frequency to about 80 kHz.

Figure 6a shows the high-temporal-resolution time traces of the plasma potential measured by BPP, the LP floating potential, and the electron temperature at $r = 3.5$ cm. The latter is multiplied by $\alpha_{LP} = 4$ for comparison on the same scale, as suggested by eq. (2). The observed fluctuation modes demonstrate the capability of the diagnostic to capture fast plasma dynamics. Figure 6b presents the corresponding power spectral densities at the same radial position. The two floating potential spectra exhibit similar characteristic frequencies, but the amplitude of LP floating potential fluctuations is generally higher because the LP signal is also affected by electron temperature fluctuations, which display the same spectral features as the potential fluctuations. As observed, the difference between the BPP and the LP floating potential fluctuations amplitudes becomes more pronounced with increasing radius, reflecting the growing influence of electron temperature fluctuations on the LP measurements. This is also confirmed, at the plasma edge and periphery, by the measured phase-shift between the LP floating potential and the temperature being locked around 180° and their coherence approaching 1 over a wide range of frequencies.

The fluctuations at 4-5 kHz appear to be consistent with the expected drift-wave mode inferred from the local density gradient around r = 3.5 cm, whereas the 1-3 kHz modes are more likely associated with a Simon-Hoh type drift instability. This kind of instability is often detected in plasma thrusters, and it is driven by the simultaneous local existence of a density gradient and a radial electric field satisfying the condition $E \cdot \nabla n > 0$ [33-35]. This condition is indeed met in the present experiment, in the region of the PANTA plasma where the radial density gradient is largest. There, the radial electric field associated with the well-type plasma potential profile drives the required $E \times B$ drift that leads to the excitation of a Simon-Hoh type drift instability.

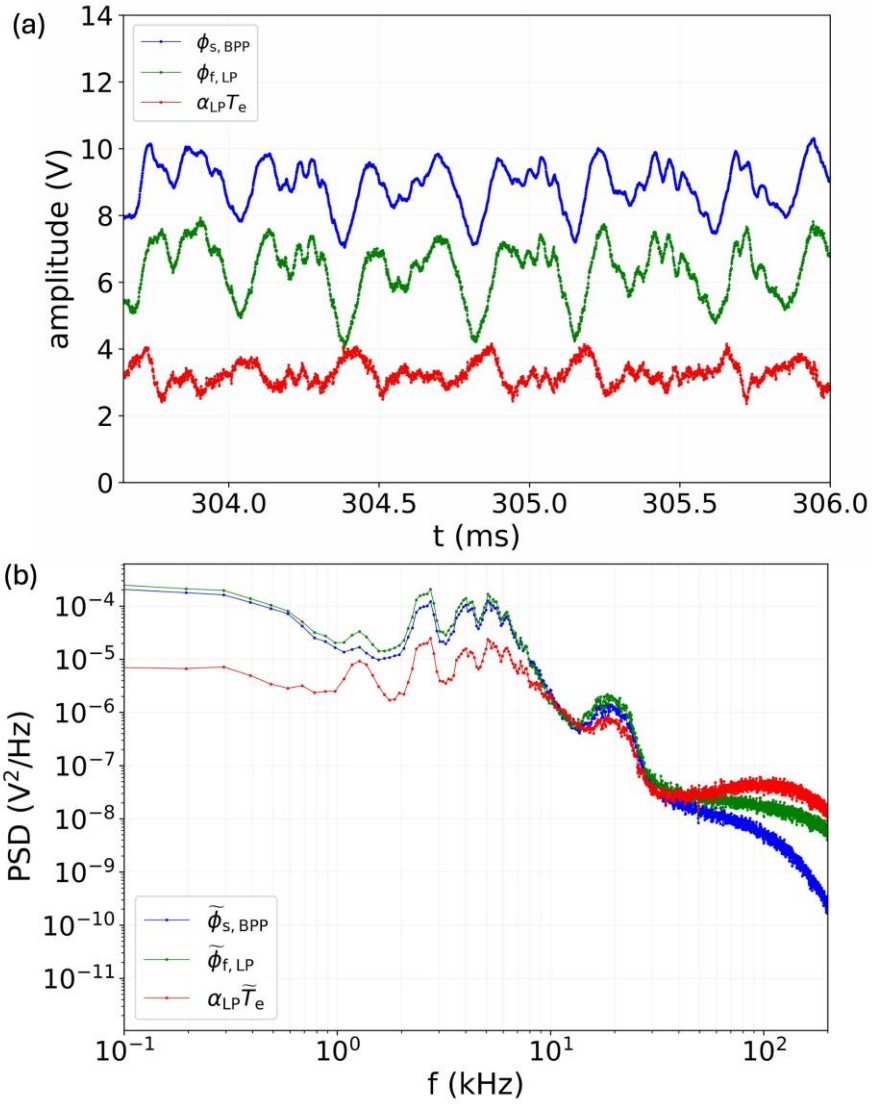


Figure 6. (a) Time traces and (b) auto-power spectral densities of the plasma potential measured by BBP (blue), the floating potential measured by LP (green), and electron temperature contribution T_e (red) multiplied by α_{LP} at r = 3.5 cm. The PSD frequency resolution is 100 Hz.

The non-linear self-coupling of the plasma potential was investigated at the same radial position through bicoherence analysis. Squared bicoherence is calculated according to:

$$\hat{b}^2(f1, f2) = \frac{|\langle X(f_1)X(f_2)X^*(f_3)\rangle|^2}{\langle |X(f_1)X(f_2)|^2\rangle\langle |X(f_3)|^2\rangle}\ , \tag{3}$$

where $X(f_1)$, $X(f_2)$ and $X(f_3)$ represent the Fourier coefficients at frequencies of f_1, f_2, and f_3 $(= f_1 + f_2)$. It quantifies nonlinear phase coupling among fluctuation components satisfying the interaction condition $f_3 = f_1 + f_2$, thereby identifying possible three-wave interactions in the turbulent spectrum [36-38].

Figure 7 shows the auto-bicoherence spectra for the floating potential signal of both LP (a) and BPP (b). Only the BPP measurements clearly reveal non-linear interactions between low-frequency fluctuations and broad band turbulent fluctuations. Both the drift wave at 4-5 kHz and the Simon-Hoh instability related to the 1-3 kHz fluctuations might be involved in the nonlinear coupling. Further investigation will be carried out with a two-channels BPP array, which can measure the spatial wavelength [39] of the instability, and prove a direct estimation of the radial electric field. Soon, the new array will be also able to measure fluctuations-driven heat and particle fluxes.

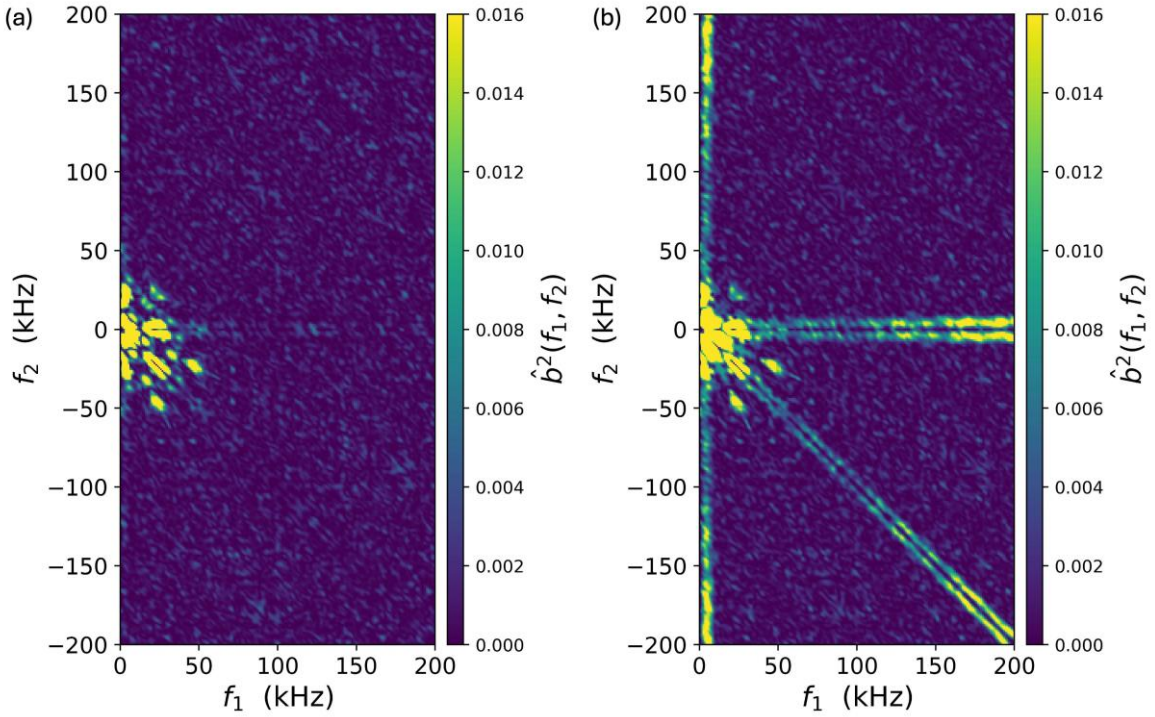


Figure 7. Auto-bicoherence of (a) LP floating potential and (b) BPP floating potential at r = 3.5 cm. The frequency resolution for this bicoherence analysis is 1 kHz (FFT size = 1024). The confidence level of bicoherence is approximately 0.0034.

IV. CONCLUSIONS

In this work, a ball-pen probe was successfully implemented and validated for the first time in a linear helicon plasma, which is widely used as a source for several applied plasma studies. In PANTA device, BPP operation enabled direct measurements of the entire plasma potential profile. Its combined use with a LP also provided the electron temperature radial profile.

The BPP successfully provided plasma potential and electron temperature measurements consistent with Langmuir probe results in the edge and peripheral region of the plasma without any correction. In the core region, discrepancies were observed and believed to be due to increased ion collisionality and reduced ion magnetization, which affect the currents balance condition required for optimal BPP operation. However, good agreement with LP measurements was successfully achieved also in the core region after applying a correction based on the BPP α coefficient. In the present experimental conditions, the BPP was found to operate reliably without correction at radial positions where the ion Hall parameter remains approximately above 0.1.

The BPP also exhibited a strong capability for investigating plasma potential and electron temperature fluctuations. BPP was able to detect temperature fluctuations coherent modes. Moreover, the initial turbulence investigation revealed the presence of a Simon–Hoh instability, a mode frequently reported in plasma-based thrusters.

Bicoherence analysis on BPP data revealed nonlinearly coupled structures that are not observable using conventional Langmuir probe measurements. The result suggest that low-frequency Simon-Hoh and drift-wave instabilities are nonlinearly coupled with higher-frequency plasma turbulence. This demonstrates that direct access to plasma potential is essential for accurately characterizing fluctuation-driven phenomena.

These experimental results confirm the potential of the BPP as a powerful diagnostic tool for investigating nonlinear dynamics in linear helicon plasmas, and ultimately, for contributing to unresolved questions regarding turbulence and anomalous transport in plasma thrusters.

Data Availability

The datasets used and/or analyzed during the current study are available from the corresponding author on reasonable request.

References

[1] Guzdar, P. N., Liu, C. S., Dong, J. Q., & Lee, Y. C. Model for thermal transport in tokamaks. *Phys. Rev. Lett.* **57**, 2818 (1986).

[2] Yuh H. Y. *et al*., Internal transport barriers in the National Spherical Torus Experiment. *Phys. Plasmas* **16**, 056120 (2009).

[3] Horton, W., Tajima T., Dong J-Q., Kim J-Y. & Kishimoto, Y. Ion transport analysis of a high beta-poloidal JT-60U discharge. *Plasma Phys. Control. Fusion* **39**, 83 (1997).

[4] Takahashi K*.,* Charles, C. & Boswell, R. W. Wave-driven electron inward transport in a magnetic nozzle. *Sci. Rep.* **12**, 20137 (2022).

[5] Yamamoto, N. *et al.* Observation of Plasma Turbulence in a Hall Thruster Using Microwave Interferometry. *J. Propuls Power* **39** (6), pp. 849-855 (2023).

[6] Koeda, A. *et al*. Numerical Simulation of Plasma Perturbations and Electron Transport in Hall Thrusters. *Trans. Jpn. Soc. Aeronaut. Space Sci.*, **68**, 2, pp. 114-121 (2025).

[7] Tange, T., Inoue, S., Itoh, K. & Nishikawa, K. Anomalous Transport Due to Electromagnetic Fluctuations across a Magnetic Field. *J. Phys. Soc. Jpn.* **46**, 1 (1979).

[8] Ross, D. W., On Standard Forms for Transport Equation and Fluxes. *Comments Plasma Phys. Control. Fusion* **12**, 155 (1989).

[9] Ratynskaia, S. V., Demidov, V. I. & Rypdal K. Measurements of Anomalous Particle and Energy Fluxes in a Magnetized Plasma. *Physical Review E* **65**, 066403 (2002).

[10] Jobes, F. C. & Hickok, R.L. A direct measurement of plasma space potential. *Nucl. Fusion* **10**, p.195 (1970).

[11] Sheehan, J. P. & Hershkowitz, N. Emissive Probes. *Plasma Sources Sci. Technol.* **20,** 063001 (2011).

[12] Kin, F. *et al.* Observations of Radially Elongated Particle Flux Induced by Streamer in a Linear Magnetized Plasma. *Phys. Plasmas* **26**, 042306 (2019).

[13] Shinohara, S. Helicon High-Density Plasma Sources: Physics and Applications, *Advances in Physics: X*, **3**(1), 1420424 (2018).

[14] Shinohara, S. High-Density Helicon Plasma Science: From Basics to Applications (Springer, 2023).

[15] Adamek, J. *et al*. A Novel Approach to Direct Measurement of the Plasma Potential. *Czech. J. Phys*. **54**, C95 (2004).

[16] Katsumata, I. & Okazaki, M. Ion Sensitive Probe - A New Diagnostic Method for Plasma in Magnetic Fields. *Jpn. J. Appl. Phys*. **6**, 123 (1967).

[17] Adámek, J. *et al*. Application of the Ball-Pen Probe in Two Low-Temperature Magnetised Plasma Devices and in Torsatron TJ-K. Contrib. *Plasma Phys.* **53**, 39 (2013).

[18] Grenfell, G. *et al*. High-Heat Flux Ball-Pen Probe Head in ASDEX-Upgrade. *Rev. Sci. Instrum.* **93**, 023507 (2022).

[19] Adamek, J. *et al.* Ion Temperature Measurements in the Tokamak Scape-Off Layer with High Temporal Resolution. *Nucl. Fusion* **61** (3), 036023 (2021).

[20] Cipciar, D. *et al*. Study of Ion-to-Electron Temperature Ratio at the Edge of Wendelstein 7-X Using a Fast Swept Ball-Pen Probe. *Plasma Phys. Control*. Fusion **67**, 115029 (2025).

[21] Adamek, J. *et al*. Ball-Pen Probe Measurements in L-Mode and H-Mode on ASDEX Upgrade. Contrib. *Plasma Phys.*, **50**: 854-859 (2010).

[22] Adamek, J. *et al*. Electron Temperature and Heat Load Measurements in the COMPASS Divertor Using the New System of Probes. *Nucl. Fusion* **57**, 022010 (2017).

[23] Walkden, N. R. *et al.* Profile Measurements of the Electron Temperature on the ASDEX Upgrade, COMPASS, and ISTTOK Tokamak Using Thomson Scattering, Triple, and Ball-Pen Probes. *Rev. Sci. Instrum*. **86**, 023510 (2015).

[24] Bousselin G. *et al*. Design and Validation of the Ball-Pen Probe for Measurements in a Low-Temperature Magnetized Plasma. *Rev. Sci. Instrum*. **84**, 013505 (2013).

[25] Harris, B. J. *et al*. Ball-Pen Probe in Strongly Magnetised RF Plasmas. *Plasma Sources Sci. Technol.*

28, 055018 (2019).

[26] Zanáška, M., Adamek, J., Peterka, M., Kudma, P. & Tichý, M. Comparative Measurements of Plasma Potential with Ball-Pen and Langmuir Probe in Low-Temperature Magnetized Plasma. *Phys. Plasmas* **22**, 033516 (2015).

[27] Murphy-Sugrue, S., Harrison, J., Walkden, N.R, Bryant, P. & Bradley, J.W. Improved Understanding of the Ball-Pen Probe Through Particle-in-Cell Simulations. *Plasma Phys. Control. Fusion* **59**, 055007 (2017).

[28] Chen, F. F. Lecture notes on Langmuir Probe Diagnostics. *IEEE-ICOPS meeting* (2003).

[29] Oldenbürger, S. *et al*. Dynamics of Particle Flux in a Cylindrical Magnetized Plasma. *Plasma Phys. Control. Fusion* **54**, 055002 (2012).

[30] Di Matteo, D. *et al*. Fluctuation-Based Calibration of Probe Radial Position in Linear Magnetized Plasmas. *Plasma Fusion Res*. **21**, 1201026 (2026).

[31] Hutchinson, I. H. Principles of Plasma Diagnostic (Cambridge, 1987).

[32]Komm, M., Adamek, J., Pekarek, Z. & Panek, R. Particle-In-Cell Simulations of the Ball-Pen Probe. *Plasma Phys. Control. Fusion* **53**, 015005 (2011).

[33] Sakawa, Y. *et al*. Nonlinear Evolution of the Modified Simon-Hoh instability Via a Cascade of Sideband Instabilities in a Weak Beam Plasma System. *Phys. Rev. Lett.* **69**, 85 (1992).

[34] Boeuf, J.P. & Smolyakov, A. I. Physics and Instabilities of Low-Temperature $E\times B$ Plasmas for Spacecraft Propulsion and Other Applications. *Phys. Plasmas* **30**, 050901 (2023).

[35] Morin V. & Smolyakov, A. I. Modification of the Simon-Hoh Instability by the Sheath Effects in Partially Magnetized $E\times B$ plasmas. *Phys. Plasmas* **25**, 084505 (2018).

[36] Itoh, K. *et al*. On the Bicoherence Analysis of Plasma Turbulence. *Phys. Plasmas* **12**, 102301 (2005).

[37] Nagashima, Y. *et al.* Observation of Coherent Bicoherence and Biphase in Potential Fluctuations Around Geodesic Acoustic Mode Frequency on JFT-2M. *Plasma Phys. Control. Fusion* **48**, A377 (2006).

[38] Fujisawa, A. A Review of Zonal Flow Experiments. *Nucl. Fusion* **49**, 013001 (2009).

[39] Ichiki, R., Kaneko, T., Hayashi, K., Tamura, S. & Hatakeyama, R. Parallel-Velocity-Shear-Modified Drift Wave in Negative Ion Plasmas. *Plasma Phys. Control. Fusion* **51**, 035011 (2009).

Acknowledgements

The authors want to thank Prof. A. Fujisawa and Dr. T. Nishizawa for their precious support and are indebted to I. Niiya for his technical assistance.

Funding

This work was supported by JST SPRING Japan Grant Number JPMJSP2136, JSPS KAKENHI Grant Numbers 26K22312 and 24K06996. It was partly supported by the Collaborative Research Program of the Research Institute for Applied Mechanics, Kyushu University.

Author contributions

D. Di Matteo and C. Moon performed the experiments and analyzed the data. D. Di Matteo wrote the main manuscript text and prepared all the figures. J. Adamek, J. Cavalier, T. Yamada, R. Namimatsu, Y. Nagashima and H. Chung contributed to the discussion, the preparation and review of the manuscript. C. Moon supervised the project.

Competing interest

The authors declare no competing interests.